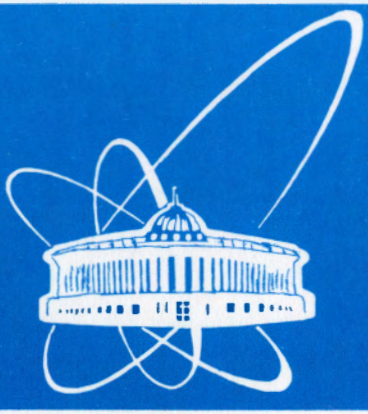

СООБЩЕНИЯ
ОБЪЕДИНЕННОГО
ИНСТИТУТА
ЯДЕРНЫХ
ИССЛЕДОВАНИЙ

Дубна

00-174

E1-2000-174

V.M.Bystritsky

MULTISENSORY EXPERIMENTS AND DATA ACQUISITION SYSTEMS ON THE MESON FACILITIES

2000

1 Introduction

To know parameters of all accompanying or competing processes is a necessary condition for increasing the measurement accuracy for characteristics of physical processes. Depending on the experimental goals, this sort of information can be provided by a variety of additional detectors, such as elementary particle and nuclear radiation detectors, electromagnetic transducers, pressure gauges, temperature sensors, humidity detectors.

The present paper describes some typical many-detector systems and data acquisition system used in the experiments at the meson factories [1] PSI (Paul Scherrer Institute, Switzerland), TRIUMF (Vancouver, Canada), LAMPF (USA), RAL (England), KEK (Japan).

The paper also presents some most important results currently obtained with the above systems. A class of experiments also is described which are aimed at investigation of very rare processes that can be observed only at high pion and muon flux densities inaccessible at classical proton accelerators (synchrocyclotron, phasotron) with a pion-producing target.

The ideology of experiments on rare processes and their data analysis should guarantee the highest possible reliability of the results. The most typical many-detector experiments for various lines of investigation at meson factories are exemplified below.

2 Muonic catalysis of nuclear reactions

Fifty years ago it was first proposed that a negative muon could catalyze the nuclear fusion reaction of hydrogen isotopes [1, 2]. This phenomenon was experimentally found by Alvarez [3] in 1957 in a mixture of hydrogen and deuterium. A hope to create an alternative source of power to be produced at room temperature arose on the basis of the hypothesis that one muon can initiate many nuclear fusion reactions of hydrogen isotopes. Essentially muonic catalysis of nuclear reactions consists in the following. When a negative muon stops in a target filled with hydrogen, deuterium, tritium, or their mixture, an excited hydrogen mu-atom with initial kinetic energy of the order of some eV is formed and then undergoes de-excitation and thermalization. Systems like this are electrically neutral, very compact (the orbit of the $p\mu$-atom has an about 200 times smaller radius than the orbit of normal hydrogen atom), and thus easily penetrate through the electron shell of other atoms coming within a distance of the order of a mesoatomic length unit ($a_\mu = 2.56 \cdot 10^{-11}$ cm) to their nuclei. This close approach allows formation of muonic molecules of hydrogen isotopes (depending on the composition of the mixture of hydrogen isotopes, $pp\mu$, $pd\mu$, $pt\mu$, $dt\mu$, $dd\mu$, $tt\mu$ molecules can be formed), where nuclear fusion reactions (dd, pd, dt, pt, tt fusion) with emission of γ quanta, neutrons, and charged particles (^{3}He, ^{4}He, p, t) may occur. As is seen, mu-atomic (MA) and mu-molecular (MM) processes in mixtures of hydrogen isotopes form a multitude of competing processes (CP) and accompanying processes (AP) with respect to the process under study. Therefore, information on characteristics of all CP and AP is also necessary to describe correctly the kinetics of the process under study. One can gain this information by using a great variety of detectors for nuclear fusion products, mu-X-ray radiation, muons and electrons from the muon decay. In the past three decades considerable study has been given to MA

[1] A meson factory is an accelerator to produce high-intensity π-meson and muon beams in a wide energy range. The maximum intensity of π-meson and muon beams, e.g. at PSI, is 10^{10} π/s and $5 \cdot 10^8$ μ/s respectively.

and MM processes arising from stops of negative muons in pure hydrogen isotopes and their mixtures [4, 5, 6, 7] at various temperatures and densities.

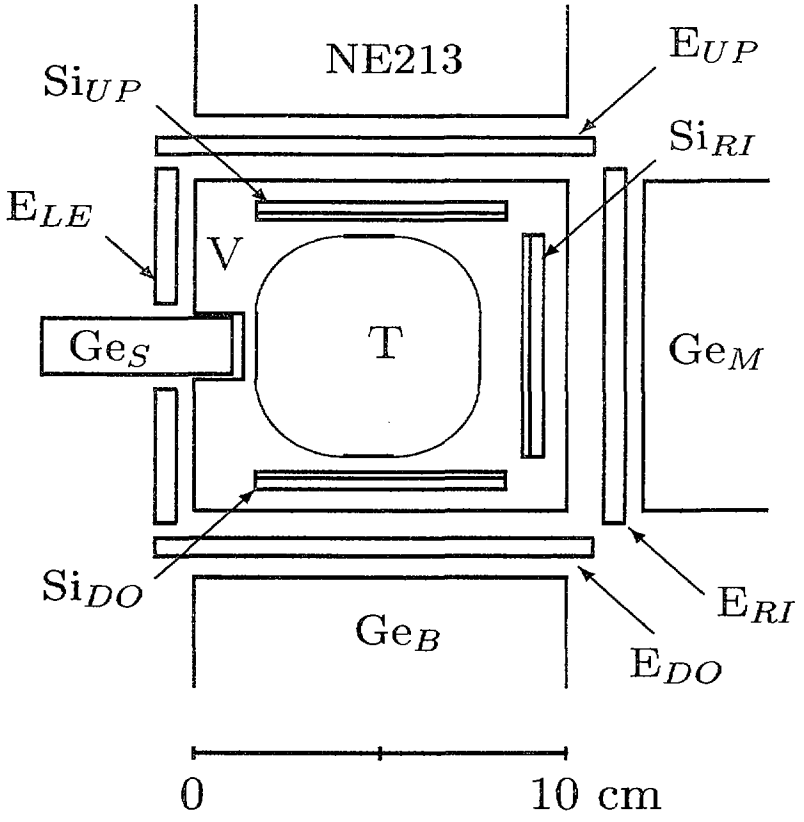

Fig. 1. The Experimental setup for investigation μ-atomic and μ-molecular processes in hydrogen- helium mixtures (dHe-experiment): Si_{UP}, Si_{RI}, Si_{DO} - Si (dE/dx - E) detector pairs located above, below and to the right of the muon beam; E_{UP}, E_{LE}, E_{DO}, E_{RI} - muon decay electron counters; Ge_S, Ge_B, Ge_M - three different Ge detectors to measure different γ - ray energies: $0 \div 20$ keV, $0 \div 1$ MeV, $0 \div 25$ MeV, NE 213 - dd fusion neutron counter with the liquid scintillator NE 213; T - gaseous target; V - vacuum chamber. Muon beam detectors 1 and 2 are not indicated.

In 1978 a Dubna team experimentally found the resonance mechanism [8] for formation of muonic deuterium molecules. In 1979 the same team was the first to find muonic catalysis of the fusion reaction of deuterium and tritium nuclei [9]. The muonic catalysis efficiency for the dt fusion reaction was found to be high: one muon stopped in the

deuterium-tritium mixture could initiate up to 200 dt fusion reactions, which corresponded a total energy release of about 3.4 GeV/μ. So much promising data allow muonic catalysis to be seriously treated as an alternative power production method [10].

This challenge has retained its topical nature up to now, but it requires solution of some technical problems, such as generation of a magnetic field with strength $10 \div 15$ T in a volume of a few cubic meters and handling of radioactive tritium of a few MCi, which themselves are sophisticated and nontrivial. Nevertheless, the investigations of MA and MM processes yielded important results of their own, characterizing a system of three bodies interacting by the Coulomb law [11, 12, 13, 14] [2].

Before listing the most important of the results, we briefly describe some typical detecting systems used in the muonic catalysis experiments.

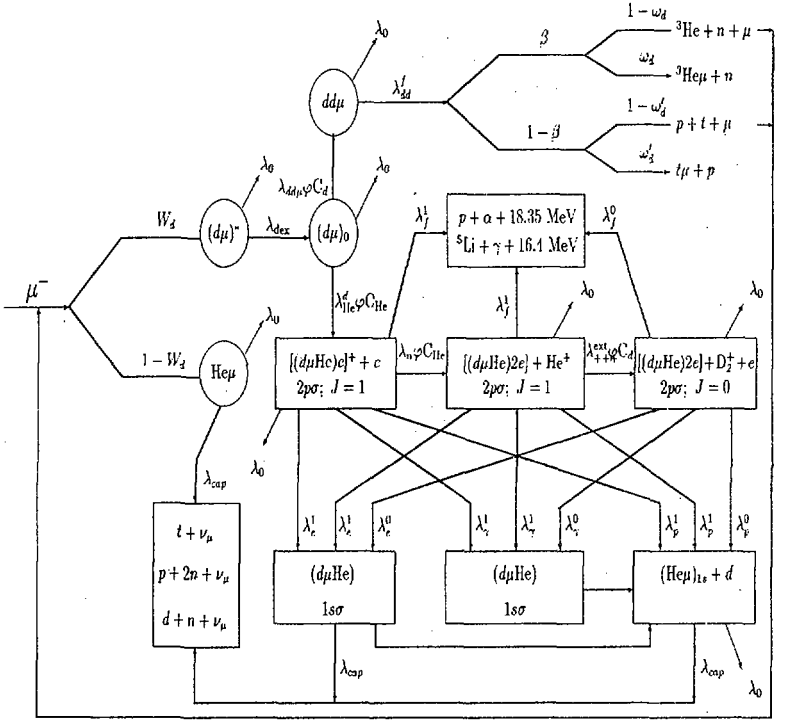

Fig. 2. A scheme of muonic processes occurring in the $D_2 + ^3He$ mixture after the negative muon stopped in it.

By way of example we consider experiments with a setup used at the meson factory at PSI (Switzerland). The setup (see Fig. 1) is designed to study fusion reactions in charge-nonsymmetrical muonic molecules dHeμ [15, 16, 17, 18, 19] and reactions of muon

[2] Comparison of the experimental and calculated data will allow a test of the solution algorithm for the problem of three bodies interacting by the Coulomb law.

capture by the He nucleus resulting in production of two and more charged products in the final state [20]:

$$d\mu^3He \rightarrow^4 He\mu + p \ \ (14.7MeV), \tag{1}$$

$$d\mu^4He \rightarrow^5 Li\mu + \gamma, \tag{2}$$

$$^3He\mu \rightarrow p + n + n + \nu_\mu, \tag{3}$$

$$^3He\mu \rightarrow d + n + \nu_\mu. \tag{4}$$

Fig.2 presents a scheme of muonic processes occurring in the D_2+^3He mixture after the negative muon stopped in it. As seen, themain competing process with respect to the investigated processes is the muon decay $\mu^- \rightarrow e^- + \nu_\mu + \tilde{\nu}_e$ (it rate is $0.455 \cdot 10^6\ s^{-1}$). The setup consists of a gas target filled with a mixture of deuterium and He (He concetration is about 5%) and a system of detectors comprising:

- three pairs of $E - \Delta E$ Si telescopes (diameter 45 mm, E detector thickness 4 mm, ΔE detector thickness 360 μm);
- eight plastic scintillator detectors of muon decay electrons arranged around the target;
- a detector of mu-X-ray radiation in the range $4 \div 10$ keV (V = 0.17 cm^3);
- a Ge detector (V = 122 cm^3) to record γ quanta in the energy range $10 \div 20$ MeV;
- a Ge detector of volume 75 cm^3 to record mu-X-ray radiation from $C\mu$, $N\mu$ and $O\mu$, atoms in the energy range $100 \div 500$ keV (in order to reveal C, N, and O impurities in the deuterium-helium mixture);
- a detector based on liquid scintillator NE 213 to record neutrons from the fusion reaction in the $dd\mu$ molecule (with energy 2.5 MeV);
- muon beam detectors on the basis of plastic scintillators.

The setup was placed in muon channel $\mu E4$ of PSI. A beam of muons with momentum P_μ = 35 MeV/c passed through monitor counter 1 (plastic scintillator $4.2 \times 4.2 \times 0.1\ cm^3$), connected in anticoincidence with another scintillation detector 2 with a 3.5-cm diameter aperture centered around the beam axis, through the entrance window of the cryostat target and stops within the deuterium- helium mixture initiating reactions 1-4. Detectors 1 and 2 are not shown in Fig. 1.

The diagram of the recording electronics trigger and the time diagram are displayed in Fig. 3a, b. The trigger signal, which was composed from a pulse from the beam entrance scintillator in delayed logical coincidence with a gate enabled by any of the active detectors, was sent to the data acquisition system when a good event was detected. The pile-up-gate (PUG) busy (B) output was set on for a 10 μs lock-out time. The barred output from the PUG (symbol $\overline{B}$), always set to the logical complement of the PUG out value, was used to indicate either that the system had accepted a muon, or was able to accept a muon. A general inhibit signal $\overline{I}$ due either to an event trigger (HINH), the computer readout time (CINH and EI), or a failure in the high voltage supply of the photomultipliers (WCINH), was combined with T1 and $\overline{B}$ signals to designate the condition when the event gate EVG could open and good events could be accepted.The

$T\overline{BI}$ signal was sent to the individual detector coincidences to permit acceptance of events,and to the CAMAC TDC units as a common start.

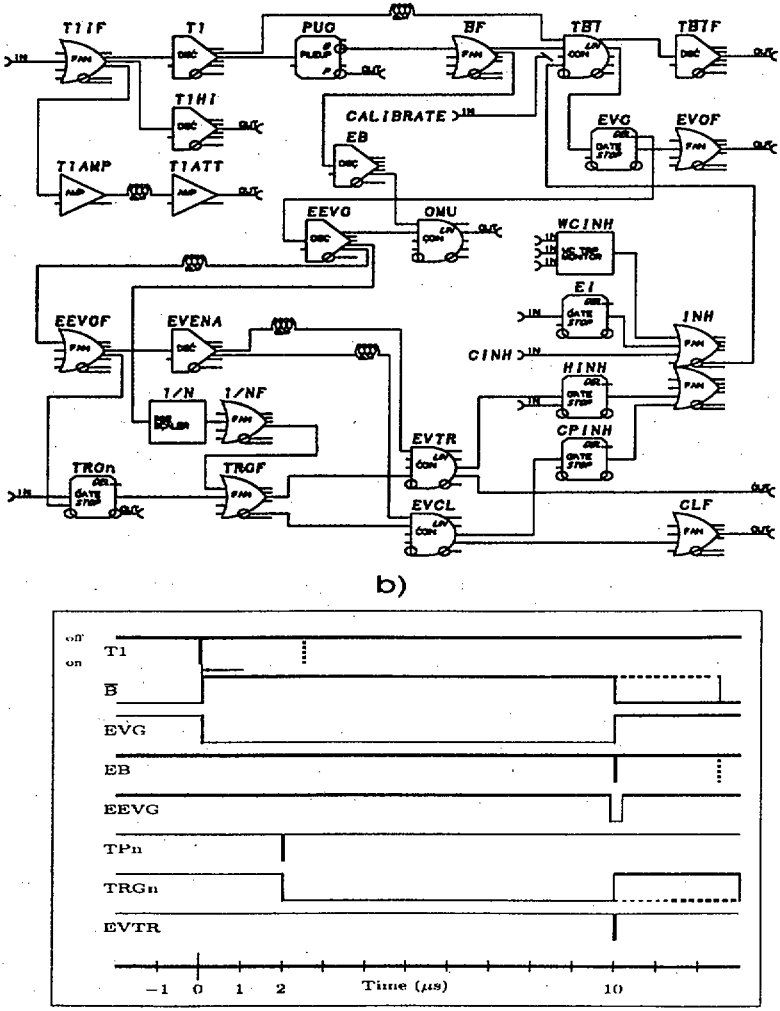

Fig. 3. a) the electronics diagram for the trigger circuit of dHe - experiment. The input to T1IF came from the beam entrance scintillator T1 and the inputs to the (generic) TRGn were supplied by the individual detectors. The critical outputs of EVGE, EVTR and EVCL were sent to the detectors electronics, data acquisition system, and CAMAC module clear inputs respectively; b) the timing setup for the electronics in the top. Time is indicated horizontally, and logic level, on/off, indicated by the lower/higher lines in keeping with NIM logic level standard.

If the second muon activated the entrance scintillator T1 (dashed event in T1 time line, Fig.3b), the PUG began timing the lock-out again,extending it.When any one of the n detectors recorded an event at a time when the EVG gate was true,such as pictured TPn in Fig.3b, a gate TRGn was opened. An event trigger would immediately initiate a hardware inhibit (HINH) to prevent loss of the data already measured by disabling the $T\overline{BI}$ coincidence. A computer-driven signal output system would maintain the inhibit while the data were read (CINH) and while the CAMAC modules were cleared (EI). An event clear would inhibit the trigger (CPINH) and the remove any values accidently recorded by CAMAC system.

One of the more important scalers was the GMU count, which was made by the coincidence of the end of busy EB and the end of event gate EEVG signals.These two signals in coincidence implied that there was no pileup and hence the muon was "good" in terms of the physics we wish to measure.

Information on the recorded event includes the time and amplitude of the signals from all above-mentioned charged and neutral particle detectors within 10 μs since the instant of operation of muon beam detector 1. As 14.7-MeV protons were recorded in the experiment, the following selection criteria for events recorded by Si detectors were used to appreciably suppress the background in the data analysis: arrival of a signal from at least one of six Si detectors within 10 μs since the instant of operation of the entrance muon counter; absence of another signal from the entrance muon detector within 10 μs; arrival of a signal from detector 1 in a certain amplitude range corresponding to the beam muons (because of electron and pion impurity in the muon beam);certain ranges corresponding to recording of protons and deuterons from reactions 1-3; arrival of an electron detector signal with an amplitude falling within a certain range at a time satisfying the criterion $t_e > t_{Si}$ (t_e, t_{Si} are the times of arrival of signals from the electron detectors and the Si detectors).

The time and amplitude distributions of the selected events (recorded by Si detectors) were compared by the χ^2 method with the theoretical Monte Carlo distributions to find the rates of processes 1-4. Note that selection of events and their further analysis are usually carried out with standard codes like PAW [21]. The data acquisition systems used in meson factory experiments will be discussed in more detail below.

By way of example, Fig. 4 and 5 display how amplitude distributions of events recorded by the Ge_S detector and Si telescopes are transformed after application of the above criteria. As is evident, the effect-to-background ratio is appreciably improved, which in turn increases reliability of the data analysis results. Events recorded by other detectors of the setup were processes in a similar way.

The setup in question was used at the above-mentioned meson factories in a lot of experiments (250-300) that yielded important results[3]. Among the findings are the energy-resonant mechanism for formation of $dd\mu$ and $dt\mu$ molecules [8, 9], muonic catalysis of the dt fusion reaction [9], the hyperfine level structure effect in mu-molecules of hydrogen isotopes [22, 23], the mechanism for molecular charge exchange of mu-atoms of hydrogen isotopes on He nuclei [24, 25], the Ramsauer-Townsend effect [26, 27][4], the limit of the Bragg scattering of muonic hydrogen from the H_2 (D_2, T_2) lattice [26, 27]. In addition,

[3]Selection of recorded events for analysis followed practically the same principles in various experiments. Only the type and number of secondary radiation detectors varied in accordance with tasks set.

[4]The scattering cross section shows a deep minimum at a certain energy of collision of $d\mu$ ($t\mu$)-atoms with the H_2 molecule. This phenomenon was first found in scattering of electrons from atoms of inert gases (Ar, Kr, Xe) [28].

a mesocatalytic method of energy production is proposed [10]; the upper limit for the nuclear fusion rate in the d^3He molecule is found [16, 17, 18, 19, 20, 21, 22, 23, 24, 25, 26, 27, 28, 29]; the value of the astrophysical S-factor in the pd interaction is found with a high accuracy, $S = 0.128 \pm 0.008$ [30], which is very important for solution of some astrophysical problems [31]; nuclear fusion rates in the muonic molecules $pd\mu$, $pt\mu$, $tt\mu$, $dd\mu$, and $dt\mu$ are measured [4, 5, 6], i.e., information on characteristics of strong interaction between light nuclei in the collision energy range beyond the reach of classical accelerators is gained [5] (this information is necessary for correct macroscopic description of the mechanism for interaction of few- nucleon systems within the framework of modern concepts [32, 33]); rates for muon capture by the proton and the deuteron from the hyperfine structure states of $p\mu$ and $d\mu$ atoms are measured (these results are important for checking four-fermion interaction universality and determining weak interaction constants [34, 35, 36]); the Lamb Shift of the n = 2 level in the $He\mu$ atom is measured [37]. Now measurements of the Lamb shift in the $p\mu$ atom are under way, which will allow the contribution to the level energy due to vacuum polarization to be found [38].

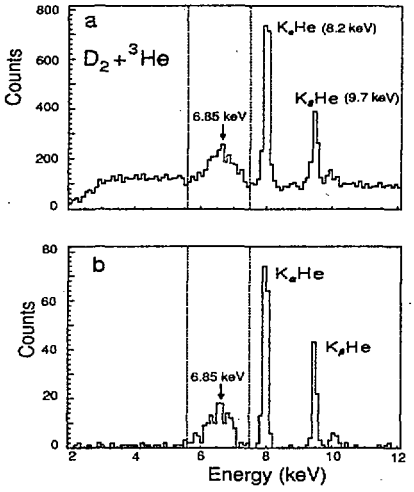

Fig. 4. Energy spectrum of the registered events by Ge_S detector when the target is fill with $D_2 + ^3He$ mixture: a, b – without and with detection of the delayed muon decay electrons, respectively.

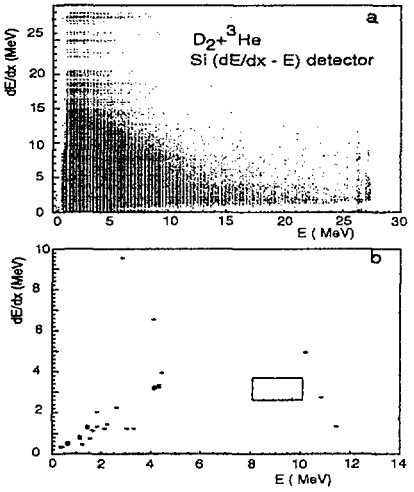

Fig. 5. Energy spectrum of all three Si detectors for $D_2 + ^3He$ mixture, without and with detection of the delayed muon decay electron, respectivelly. dE/dx is plotted versus E.

This great variety of investigations of MA and MM processes allowed various off-line software packages to be developed on the basis of combined analysis of the energy and time distributions of muon decay electrons, products of nuclear fusion reactions in muonic molecules, mu-X-ray radiation, which in turn allows reliable precise information on characteristics of processes under study to be obtained.

[5] The astrophysical range of constituent nucleus collision energies is realized in muonic molecules.

3 Search for rare decays

3.1 Introduction

Study of rare processes is a priority trend in the research at meson factories. Among these processes are muonium-to-antimuonium conversion ($\mu^+e^- \to \mu^-e^+$); $\mu \to e$ conversion in the process $\mu^-A \to e^-A$; decays $\mu \to e + \gamma$, $\pi^+ \to e^+ + \nu_e$, $\mu \to 3e$, $\pi^+ \to \pi^0 + e^+ + \nu_e$. According to estimations, probabilities for these processes are as low as $10^{-13} \div 10^{-16}$ against the basic muon or pion decay modes. Interest in the study of these processes arises from the necessity to test modern particle physics models.

It is an aim of physics to understand the fundamental laws of matter and the forces which hold matter together.Experiments are done to investigate the existing models and to show their validity. Deviations from predictions of existing theories lead to change extensions of these or to completely new ideas about the laws of nature.The last three decades of elementary particle physics were marked by great successes of gauge theories in several domains: the Glashow-Weinberg-Salam theory [39] succeeded in unifying the electromagnetic and week interactions, and quantum chromodynamics gave a description of the strong force. This, so-called standard model, was subject to a large number of experiments of different kind, and the predictions of the standard model agreed with the measured quantities.

Below we describe some of the performed (planned) experiments on testing the Standard Model of particle physics and searching for new physics.

3.2 Muon-Electron Conversion(Sindrum II experiment)

3.2.1 Introduction

Observation of muon to electron conversion would be the first evidence for a process violates muon and electron type lepton number and that cannot be explained by the Standard Model of particle physics, extended to include massive neutrinos. Tests of lepton-flavor conversation (LFC) are very sensitive probes of new physics beyond the Standard Model of particle physics [40, 41] . One of the most stringent tests is the search for the neutrinoless coherent muon electron conversion in muonic atoms (A=mass number, Z=proton number):

$$\mu^- + (A, Z) \to e^- + (A, Z). \tag{5}$$

Only the coherent fraction of $\mu \to e$ conversion is of interest because then the signature is a single electron with characteristic energy

$$E_e = m_\mu c^2 - B_\mu - R_{nucl}, \tag{6}$$

where m_μ is the muon mass, B_μ is the binding energy of the muonic atom in 1s state and R_{nucl} is the recoil energy of the nucleus. Therefore the energy of the emitted electrons from the target has to be measured in a search for $\mu^- \to e^-$ conversion[6].

Below we describe the $\mu \to e$ experiment with spectrometer SINDRUM II performed at PSI [42, 45].

[6]For really used Ti and Al targets the conversion electron energy is close to the muon rest mass m_μ = 106.5 MeV.

3.2.2 Experimental setup

The setup of the spectrometer SINDRUM II is shown in Fig.6. The muon beam with an average intensity of $9 \cdot 10^6$ μ/s is analyzed in scintillation beam counter, degraded and stopped in a titanium target.

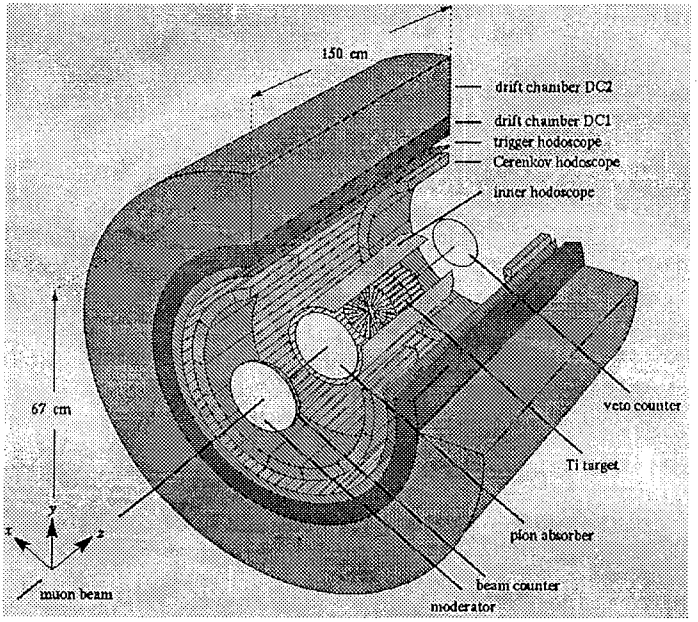

Fig. 6. Setup of the spectrometer SINDRUM II for $\mu^- \to e^-$ conversion.

The signals from the the beam counter are used for the suppression of background from pions and electrons in the beam. A superconducting solenoid produces a magnetic field which is parallel to the beam axis in a cylindrical volume 180 cm length and 67.5 cm radius. This geometry allows to use the cylindrical detectors which facilitates the trigger electronics and the offline analyses. For a magnetic field 1.2 T a $\mu \to e$ conversion electron, which has a momentum of 104.3 MeV/c, is contained within the radius of 67.5 cm. The time is measured with a cylindrical 64 element plastic scintillator hodoscope ($1500mm \times 33.75mm \times 3mm$) which has an inner radius of 34.6 cm and a thickness of 3mm.The scintillator hodoscope is also used for triggering.

Two drift chambers measure the trajectories of the emitted electrons outside the hodoscope.The first drift chamber(DC1) makes precise measurements of two track segments per revolution of the trajectories.DC1 contains 384 sense wires which measure r and ϕ coordinates. The outer wall of the chamber is covered with 192 cathode strips split in the

middle (z=0) into 192 upstream and 192 downstream strips. With the induced signals of the strips three-dimensional space points of the trajectories are reconstructed. The second drift chamber (DC2) is used to connect the two track segments of a revolution of the helical trajectories of emitted particles measured by DC1 and to recognize cosmic ray background.The drift region of DC2 is separated from amplification region. The amplification region consists of 96 aluminium modules with 6 sense wires and two guard wires. Since a granularity of 96 channels is sufficient in DC2 all six sense wires of one module are electrically connected together and define one read-out cell.

At both ends of spectrometer there are rings of 16 plexiglass Cherenkov detectors (345 mm length with trapezoidal cross section which has baselines of 107.0 mm and 118.7 mm and a height of 30 mm) inside the scintillator hodoscope which are used for triggering. The time resolution of the hodoscope is 0.8 ns (FWHM) per track. The momentum resolution of spectrometer is 2.3 %(FWHM) at p= 100 MeV/c which is dominated by the energy losses in the target. The solid angle covered by spectrometer is $0.82 \cdot 4\pi\ sr$.

With a total acceptance of 14.5 % including all inefficiencies, for detecting $\mu \rightarrow e$ conversion a total of $7 \cdot 10^{12}$ captured muons is needed to reach a sensitivity of 10^{-12} per event.

3.2.3 Electronics

Fig.7 shows a block-diagram of the read-out electronics and data acquisition computers of the SINDRUM II spectrometer. Signals coming from the scintillator hodoscope and Cherenkov hodoscope are processed using CAMAC and read out by the STARBURST [46], whereas the signals from the drift chambers and the beam counter are read out by GPM [47] ("General Purpose Master") using mainly FASTBUS.

The FASTBUS data are transfered to CAMAC via the CFI (CAMAC/FASTBUS) interface [48].The CFI is also used as an online filter. The CFI consists on the FASTBUS side of a dedicated microprocessor that accepts commands from and sends data to a CAMAC I/O unit (CFICC) over a private bus. All data are collected by the STARBURST processor.

The anode signals of the drift chambers DC1 and DC2 and the cathode signals of DC1 are read out with chain which consists of preamlifiers, postamlifiers, discriminators and TDCs. The 128 analogue signals of the scintillator hodoscope and 32 signals of the Cerenkov counters are discriminated in the discriminator - meantimers by a "high-low" threshold method. The times of the 128 scintillator and 32 Cherenkov counter discriminator output signals are measured by TDCs (LeCroy 2228A) with a resolution of 50 ns/channel.

The start times for the TDCs and the ADC gate are provided by the first level hardware trigger. In the second level, programmable FASTBUS modules (the so-called "CPS") performed a check on the event topology.

The second level hardware trigger makes uses of a programmable delay generator(PDG 4222).The delay generator is started by the first level hardware trigger and produces delays which are used as stop signals for the drift chamber TDSs and the beam counter waveform digitizer. The PDG produces the start signal for third level trigger which is the interrupt signal for the GPM.

The third level trigger is a software filter. After a GPM start signal has arrived, the GPM reads out the FASTBUS components the frond end electronics. For accepted events, the "GPM YES" signal produces the LAM signal, which creates an interrupt in the STARBURST online computer. The analogue signals of the scintillator and Cerenkov

counters are integrated during a time gate of 50 ns with ADCs (LeCroy 2249A) which have a resolution of 0.25 pC/channel.

The trigger was sensitive to electrons with a momentum of about 100 MeV/c which reach DC2 and produce at least two track elements in DC1. The beam counter signal is combined by time gates with the first level hardware trigger signal, and is sent to the digital oscilloscope (LeCroy 9450) which serves as a waveform digitizer (ADC 8 Bit/channel, time base 2.5 ns/channel.

SINDRUM II is the first experiment that used the data acquisition system TANDEM which has been developed at PS1 [49]. The front end side of the SINDRUM II data acquisition splits into two branches which may be called "CAMAC" and "FASTBUS" branches according to the data bus involved. The back end computer MicroVAXII and writes it on disk or tape. An ATARI 1040 ST computer controls the high voltage (HV) power supply for the drift chambers. The data are read out via the GPIB port (IEEE-488) of the LeCroy 9450 and a specially developed interface to the parallel port of the GPM.

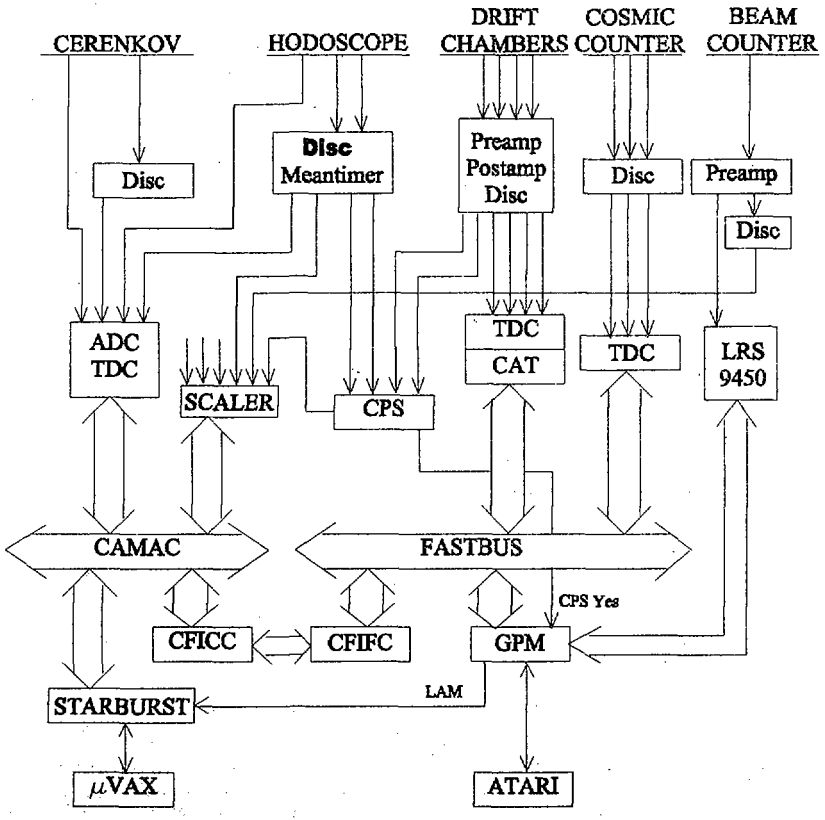

Fig. 7. Block diagram of the read-out electronics and the data acquisition system in $\mu^- \to e^-$ experiment.

3.2.4 Data analysis. Results

The result of a particle physics experiment is a sample of events, each of them characterized by a set of variables $\vec{x}$ (e.g. kinematical variables). The analysis has to determine the true distribution $f(\vec{x})$ of these variables and to compare these to the theory. A characteristic of such experiments is that mostly the distributions $f(\vec{x})$ cannot be measured directly. The distribution are modified by the detector acceptance and resolution. Generally one measures track parameters $\vec{y}$ and their distributions $g(\vec{y})$ instead of the original distributions $f(\vec{x})$.

The experiment can still be compared with the theory by applying one of the two following procedures:

- one tries to unfold the measured distributions $g_{exp}(\vec{y})$ to derive the original distributions $f_{exp}(\vec{x})$. These can be directly compared with theory and with other experiments.
- In the second method, the theoretical distributions $f_{theo}(\vec{x})$ are folded with the detector response function $f_{theo}(\vec{x}) \rightarrow g_{theo}(\vec{y})$ and then the theoretical prediction for the distributions $g_{theo}(\vec{y})$ can be compared with measured distributions $g_{exp}(\vec{y})$.

The detector response function can only be derived with Monte Carlo methods. The complete experiment is simulated on a computer. The simulation is based on the CERN programme GEANT [50].

As a result of data analysis the upper limit for the branching ratio $B_{\mu e}$ (for $\mu \rightarrow e$ conversion with respect to the rate for the ordinary muon capture) at 90% confidence level is obtained:

$$B_{\mu e} < 6.1 \cdot 10^{-13}.$$

This result is an independent confirmation of the previous best result ($4.6 \cdot 10^{-12}$) which was measured by experiment at TRIUMF [51].

There is a project of a $\mu \rightarrow e$ experiment with a specially formed muon beam to be carried out at BNL [52]. According to this project, the upper limit for $B_{\mu e}$ can be decreased by three orders of magnitude.

3.3 Pion Beta Experiment

3.3.1 Introduction

The PIBETA experiment will pursue a precise measurement of the rare pion beta decay ($\pi^+ \rightarrow \pi^0 e^+ \nu_e$) rate with an accuracy of about 0.5 %. Thanks to low theoretical uncertainties the latter can be used to constrain Cabbibo-Kobayashi-Maskawa (CKM) unitary and certain aspects of physics beyond the Standars Model [53, 54, 55]. The best experimental value at present has error limits of 4% (TRIUMF [56]) far exceeding the theoretical uncertainty of < 0.15 %.

3.3.2 Set up

The experiment (see Fig.8) will be performed at the $\pi E1$ beamline at PSI. This beamline turned to 116 MeV/c π^+, will give the necessary pion rate of up to $2 \cdot 10^6$ π^+/s with a low contamination of muons, positrons and protons. Due to the Michel positron background, the detector must be very efficient in the π^0 detection and have excellent background

suppression. The heart of the detector is a 3π spherical calorimeter consisting of 240 pure CsI crystals (see Fig.7). The central part of the apparatus contains active beam degrader and pion stopping target counters, surrounded by a charged particle (CP) tracking system consisting of a 20-bar scintillator hodoscope and a pair of concentric cylindrical wire chambers (MWPC1 and MWPC2).

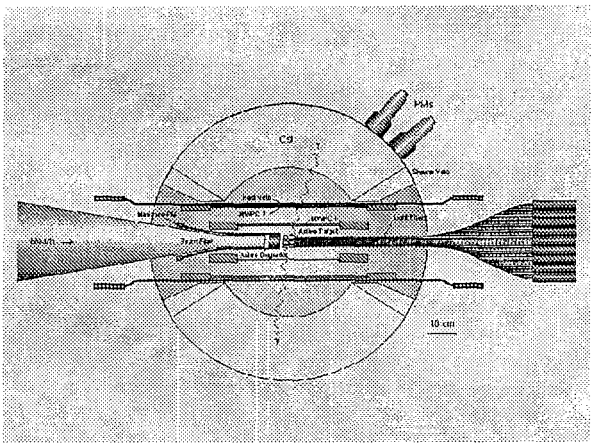

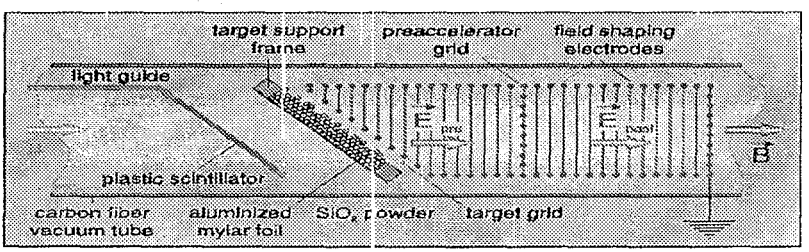

Fig. 8. Layout of the Pion Beta Detector for investigation of the $\mu^- \to e^- + \nu_\mu + \tilde{\nu}_e$ process.

3.3.3 Experimental setup

3.3.4 Data acquisition System MIDAS

This section deals with the Maximum Integrated Data Acquisition System (MIDAS) [57] which will be used in the projected experiment and is being successfully used in experiments at the meson factories PSI and TRIUMF.

The MIDAS library contains routines for buffer management, a message system, a history system and an online database. MIDAS buffers are FIFOs which support multiple

producers and multiple consumers. Consumers may request a certain subset of event types from a buffer. The transfer speed between a producer and a consumer is on the order of 10 MB/s for local access and 980 kB/s for remote access over standard ethernet. The history system is used to store data on a hard disk and produce value-over-time plots. The online database is a central data storage which contains all variables of an experiment like logging channel information, event definitions, slow control variables, front-end parameters and histogram definitions. It is kept entirelyin shared memory for fastest access of up to 50000 read/writes per second locally and 500 read/writes remotely. Several applications have been written using the MIDAS library. A general purpose logger supports multiple logging channels to disks and tapes. Different logging channels can receive different types of events in different formats. Currently three data formats are supported: ASCII, an optimized MIDAS format and the YBOS format. A command-line based editor has been created which can be used to change values in the online database interactively and to perform run control. A graphical implementation of that program using the Java language is also available. This makes it possible to control an experiment from any computer running a Java capable browser.

The PiBeta Analyzer is a computer program which can analyze data produced by the PiBeta detector. The analyzer consists of two parts: a system part which is responsible for reading/writing events in various formats and a user part which actually does the experiment specific data analysis. In order to make data analysis more flexible, a multi-stage concept has been chosen for the analyzer. A raw event is passed through several stages in the analyzer, where each stage has a specific task. The stages read part of the event, analyze it and can add the results of the analysis back to the event. Therefore, each stage in the chain can read all results from previous stages. To reflect the multi-stage concept in the data structures, a bank system is used for event storage. The online system produces banks for different parts of the detector, like a ADC bank, a TDC bank, a scalar bank and so on. The first stages in the analyzer will use these banks to produce calibrated data like energy deposition in MeV in an "calibrated ADC" bank, track position in mm in a "MWPC" bank and so on. User's can at the end add private banks which contains variables they are interested in. Since the contents of banks is defined in a database, the system part of the analyzer knows how to interpret the contents of an event. This way, N-tuples can be booked automatically by the system. When running off-line, column-wise N-tuples are used. Each bank is booked as a "block" in an CWN-tuple. The id of the CWNT is the same as the event id.

The Fig.9 shows the relationship between programs on different computers and the online Database/Buffer Manager. In the Pion-Beta Experimen two PCs are used as front-end computers connected to CAMAC, Fastbus and a LeCroy LRS1440 high voltage system. Using polling under MS- DOS an average trigger response time of 8us has been achieved. Several PC plug-in cards are used to read temperatures and gas flows. Two additional PCs are used as back-end computers running different analyzers under Windows NT. Data are written to two DLT tape units in parallel. The analyzer can read data from files, tapes or the online DAQ system. It can write events or specific banks inside events to output files. The analyzer supports currently three different file formats: MIDAS binary (.mid), pure ASCII files (.asc) and HBOOK rz files (.rz) with column-wise N-tupels and row-wise N-tuples. While the rz file format can only be used for the analyzer output, .mid and .asc files can also be read by the analyzer. Additionally, these files can be written and read directly in GNU-zipped format (.asc.gz and .mid.gz). The data is compressed and decompressed on-the-fly. While this method saves about 50% of disk space, it takes about 20% more CPU time to decompress .gz files.

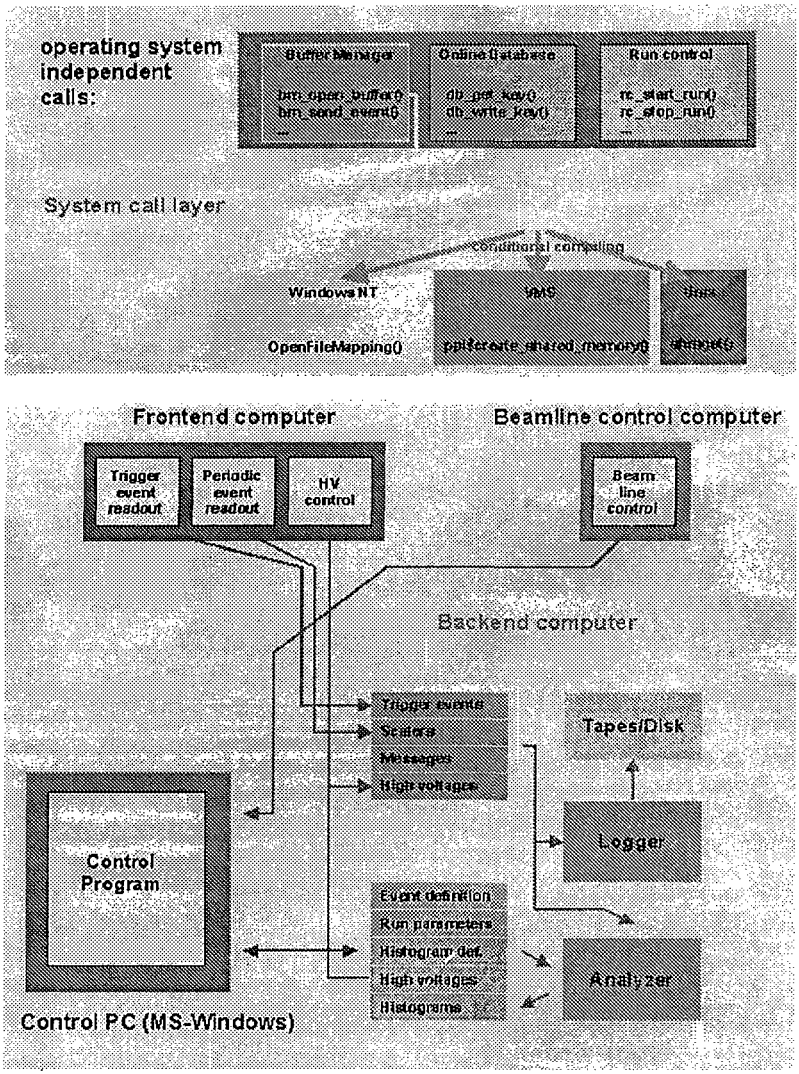

Fig. 9. The relationship between programs on different computers and the Online DataBase/Buffer Manager (Maximum Integrated Data Acquisition System).

3.3.5 Results

First calibration and commissioning data with the whole PIBETA detector were taken during a six-week long summer 1998. The analysis of the commissioning run data as well as instrumental improvements and fixes are under way.

3.4 Muonium -Antimuonium Conversion Experiment

3.4.1 Introduction

The search for the spontaneous conversion of Muonium ($M = \mu^+e^-$) to Antimuonium ($\overline{M} = \mu^-e^+$) is a sensitive method for testing new physics. This reaction violate separate additive muon and electron number conservation. Consequently, it is not provided in the standard model of electroweak interactions as are all other lepton flavour violating processes. However, in many models developed to derive some of the parameters of the standard model from fundamental principles, lepton flavour violation appears to be natural [58].

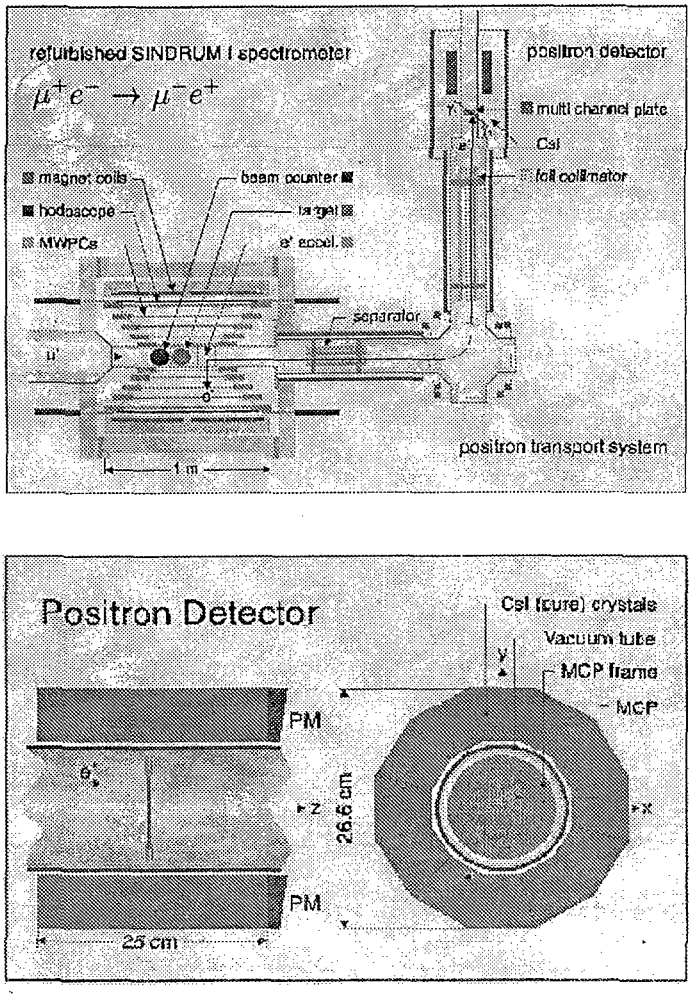

Fig. 10. Muonium - Antimuonium Conversation Spectrometer (schematic view).

In particular, some left-right symmetric models [59] and supersymmetric models with broken R-parity [60] allow muonium-antimuonium conversion with a strength $G_{M\overline{M}}$ of the order of 10^{-2} of the weak interaction strength G_F. At present, the best upper limits established in a series of experimental approaches using different techniques published for the coupling $G_{M\overline{M}}$ are 16 % and 13 % of G_F, respectively. The former experiment has been performed at LAMPF [61] the latter at Dubna [62].

The experiment at the Paul Scherrer Institute (PSI) has aimed for a sensitivity to yet undiscovered interactions with an effective coupling as small as a few permille of the Fermi coupling constant G_F, which corresponds to a sensitivity improvement by more than a factor of 1000 in comparison with the LAMPF and the Dubna experiments.

3.4.2 The Muonium-Antimuonium-Conversation-Spectrometer MACS

The schematic view of the MACS is presented on Fig.10. Muonium atoms in the ground state are formed by electron capture after stopping a subsurface beam of positive muons (momentum less than 26 MeV/c) in a silicon dioxide powder target with $\sim$ 60 % efficiency. Some of these atoms (5%) emerge from the target with thermal kinetic energies into the surrounding vacuum where an eventual transition to antimuonium is not suppressed as it is in matter (mainly due to the removal of degeneracy between muonium and antimuonium). Both constituents of antimuonium (muonium) are identified as the atoms decay. MACS is designed to identify both constituents of the antimuonium (muonium) atom after its decay. The disintegration of the atom is due to muon decay with the dominant channel $\mu^- \rightarrow e^- + \nu_\mu + \bar{\nu}_e$. The particle in the atomic shell has negligible ($< 10^{-6}$) influence on the decay process. Electrons (positrons) from muon decay have a characteristic energy spectrum ranging up to 53 MeV. In this experiment they are detected in a magnetic spectrometer operated at 1kG which allows to reconstruct the particle's momentum and sign of charge. The spectrometer consists of 5 cylindrical concentric Multi Wire Proportional Chambers (MWPC) surrounded by a plastic scintillator hodoscope located inside a solenoid magnet, which produces a homogeneous (1%) magnetic field of 0.1 T. Five chambers are equipped with helical cathode strips to allow a measurement of axial coordinates. From the measured hit coordinates the path of the particle can be reconstructed yielding its momentum and charge sign. The hodoscope consists of 64 plastic scintillator strips, each read out by photomultipliers on both ends. It is used in the trigger and as time marker for the decay process as the start of the Time of Flight measurement for the atomic shell particle. The particle from the atomic shell has a mean energy corresponding to a Rydberg energy of 13.5 eV (spectrum). It is electrostatically accelerated ($\sim$ 8 keV) and guided by a magnetic transport system to a position sensitive "positron" detector which is able to detect electrons as well. Impact time and position are recorded with a MicroChannel Plate (MCP). For the identification of positrons a segmented crystal detector surrounds the MCP to detect their annihilation radiation. The MCP assembly consists of two plates of 89 mm diameter (sensitive area 75 mm diameter) each and with resistive anode readout. The efficiency of commercial plates of 16% for 8 keV electrons and positrons could be enhanced to 64% using a MgO-coated carbon foil emitting secondary electrons in front of it.The barrel shaped crystal spectrometer surrounding the MCP is made of pure CsI and consists of 12 segments read out with magnetic field insensitive photomultipliers. Positron annihilation photons of 511 keV are detected by two segments in opposed hemispheres of the detector. The acceptance for at least one of the annihilation photons was measured to be 79% using a Na-22 radioactive source.

This experiment was carried out with the same data acquisition system MIDAS as the experiment PIBETA [57].

3.4.3 Results

An upper limit on the conversion probability in an external magnetic field of 0.1 T was obtained [63]

$$P_{M\overline{M}}(0.1T) < 8.3 \cdot 10^{-11} \qquad (90\% C.L.)$$

representing an improvement of the LAMPF result by a factor of 2740.

The new bound has been turned into an upper limit for the coupling constant $G_{M\overline{M}}$ of a hypothetical $M - \overline{M}$ interaction:

$$G_{M\overline{M}} < 3 \cdot 10^{-3} G_F \qquad (90\% C.L.).$$

The new upper limit increases the domains of validity of the standard model by postponing the scale of new physics to higher energies. In the future, significant improvements in sensitivity are conceivable, of enhanced muonium production (in vacuo) becomes feasible and/or high intensity pulsed muon beams are available.

4 Precision Measurement of the Michel Parameters of Muon Decay

4.1 Introduction

The standard model of subatomic particles and interactions purports to provide an exact description of the muon decay spectrum. This is the same model which describes the interactions and indeed the existence of the quarks, and which has been incredibly successful in describing a wide variety of subatomic phenomena. In spite of this success, it is widely believed that the theory is only approximately correct. Muon decay is a particularly interesting phenomena, In particular, the quarks are not involved in this decay. Because of this, the "strong" interaction does not play a role, which makes possible an exact quantum treatment of the decay. Furthermore, the decay is thought to respect certain symmetries. In particular, the neutrinos which are emitted are expected to have an angular momentum which is always directed opposite to the linear momentum. This "feature" of the standard model has been incorporated by fiat. There is no a priori reason to expect that neutrinos violating this symmetry principle cannot exist. If they do exist, it would be taken as evidence of an additional component of the Weak Interaction, mediated by a new particle which would be referred to as a right- handed W gauge boson. It is likely that a careful examination of the muon decay spectrum would be the best test for the existence of such "right-handed" interactions. It is remarkable that to date, a precise measurement of the entire decay distribution has not been undertaken. In TRIUMF proposal E614, "A Precision Measurement of Muon Decay Parameters " [64] it is proposed to make a precise measurement of the muon decay distribution for the purpose of determining the electroweak coupling constants which determine the underlying symmetries. Deviations from the expected decay distribution at the level of 1 part in 10000 could reveal flaws in the standard model - such as yet undetected "right-handed" interactions.

The scientific impact of such a discovery would be enormous, competing in impact with the biggest of the collider experiments.

4.2 Experiment

The drawing of the experimental setup is shown in Fig.11. The measurements will employ a large bore superconducting solenoid magnet. The $\sim$ 100% polarized 4.1 MeV surface positively charged muons produced at TRIUMF will be directed into the 2T magnetic field where they will be stopped at the centre of a precision detector package. After an individual muon is stopped in the target, (aluminium foil the tracking system is watched for several micro-seconds. If a muon decay event is observed, the positrons from the decay spiral outward in the magnetic field. By observing the angle through which the positron is.emitted and measuring the radius of curvature of the track in the magnetic field using precision wire chambers, (WC Detector Package) the angular and momentum distributions of decay events can be reconstructed.

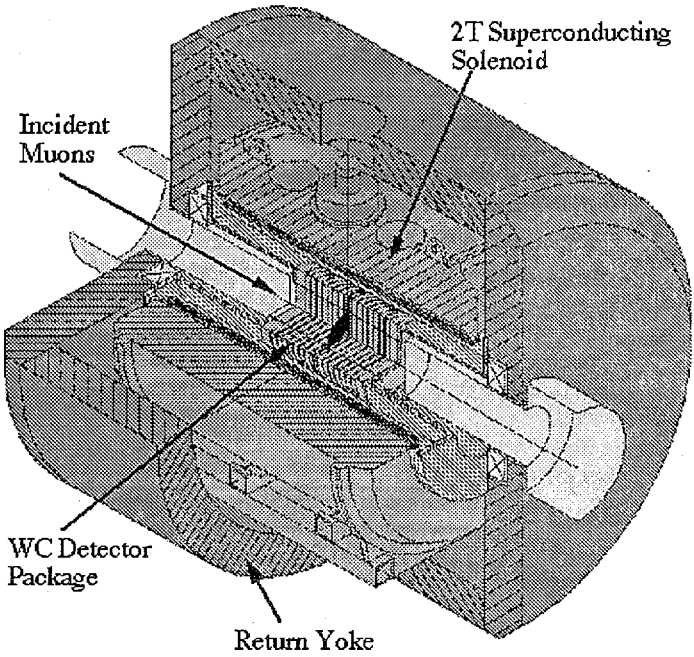

Fig. 11. The Experimental Setup for measurement of the Michel Parameter at TRIUMF.

The complete array of WC Detector Package consists of a 26 planar drift chambers and 6 proportional chambers.There are two thin($\sim$ 85 mg/cm^2) silicon counters(SiLi):the upstream one to detect the incoming muons and the downstream one to preserve symmetry. By carefully controlling systematic uncertainties in the experiment, and by collecting data

from a sample of 10^9 decay events, the decay distributions can be studied at an accuracy of less than one part in 10000. This accuracy heightens our sensitivity to various effects, including the possible existence of right-handed interactions.

MIDAS [57] is used for data collection in this experiment. At present time the experiment in progress.

5 Proposal - A Precision Measurement of the Positive Muon Lifetime Using a Pulsed Muon Beam and μ Lan Detector

5.1 Introduction

It is proposed [65] to measure the positive muon lifetime to a precision of 1 part in 10^6 giving an absolute uncertainly on the level of 2 ps. This represents more than an order of magnitude increase in precision beyond the current world average. The muon lifetime is used to determine the Fermi coupling constant, G_F, which is the fundamental quantity governing the strength of any electroweak process. Recent theoretical work [66] enables a clean extraction of G_F, from τ_μ and paves the way for a new high-precision measurement. Such an undertaking is challenging and in keeping with a recent trend to improve the precision on the knowledge of the fundamental parameters of the Standard Model to the extent that modem technology permits.

A 1 ppm determination of τ_μ requires 10^{12} muon decays. An intense muon source and a detector system capable of handling multiple events at once are required in order to acquire the data in a relatively short running period (e.g., one month).This experiment, having been designed from the start to utilize a pulsed beam, is ideally suited for a chopped surface muon beam at PSI. The experiment is designed to address specifically the known critical sources of systematic error. A depolarizing sulfur target is used to stop the μ^+ and to reduce the residual polarization of the ensemble to a few percent. Individual muon spins are dephased during the accumulation period by the inclusion of a 75 G transverse magnetic field. Decay positrons are registered in the μLan (Muon Lifetime Analysis) Detector (see Fig.12) which consists of 180 independent triangular timing tiles distributed uniformly within the 20 Super Triangles of an icosahedral geometry centered on the target. Each tile consists of an inner and an outer scintillator coupled to independent photomultiplier tubes (PMT). The inner and outer scintillators have a thickness 6.35 mm and 3.175 mm, respectively. A gap of approximately 7 mm is maintained between each tile so that no positron from any edge of the target can cross from the inner scintillator of one tile into the outer scintillator of an adjacent tile. The light from the outer scintillator is transported to a PMT through a solid, UV-Absorbing (UVA) tapered lightguide whose length is sufficient to stop the most energetic decay positrons. A system of 500 MHz waveform digitizers are used to read out each PMT. This enables both timing and energy deposition to be recorded for each event. The high segmentation and the double-pulse rejection capabilities reduce the effect of pileup on the measured lifetime to a level below 1 ppm. The geometry features 90 point-like symmetric tile pairs; the sum of any pair is used in the lifetime analysis. The difference in rate versus time in any tile pair reveals sources of asymmetry.

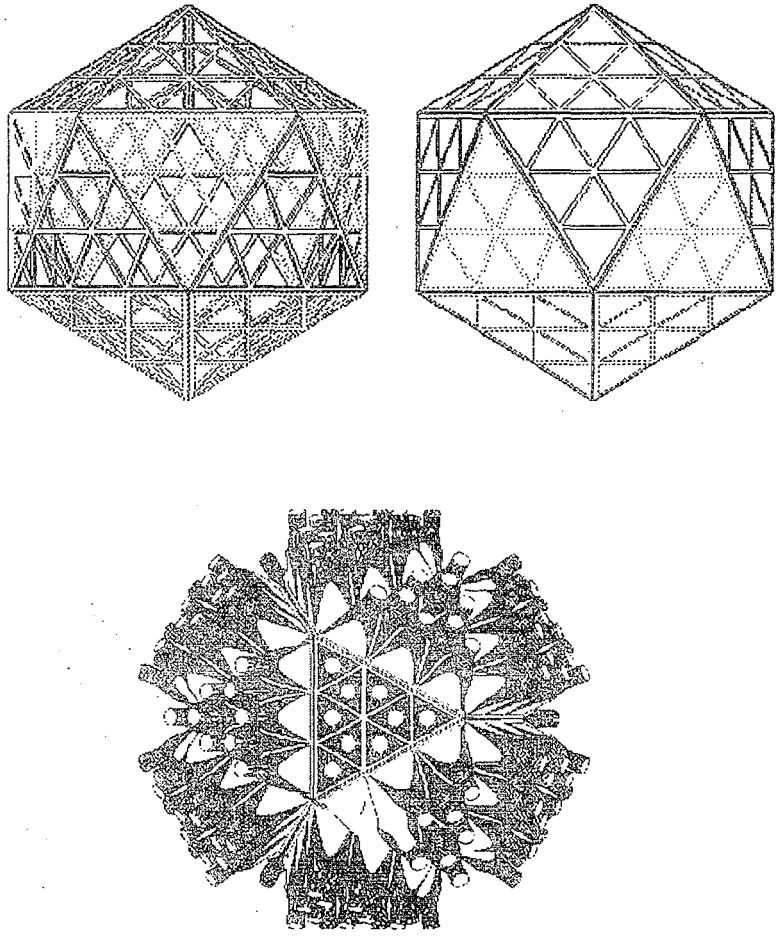

Fig. 12. The Muon Lifetime Analysis Detector.

5.2 Electronics

The task of the front end electronics is to provide timing and pulse height information for signals produced by decay positrons in the two layers of scintillating tiles. All data will take using waveform digitizers connected to every channel. In addition to the basic experimental measurement, both pulse height and timing information will be used to suppress and correct for pulse pileup. The data acquisition system must be able to read out 360 channels of phototube signals, one signal from each of the two layers of 180 tiles. The signals from front and back sections of each tile will sit on the same analog line, with

the back signal delayed by 40 ns. To keep the beamtime required to a minimum, front end acquisition and readout to tape will proceed in parallel.

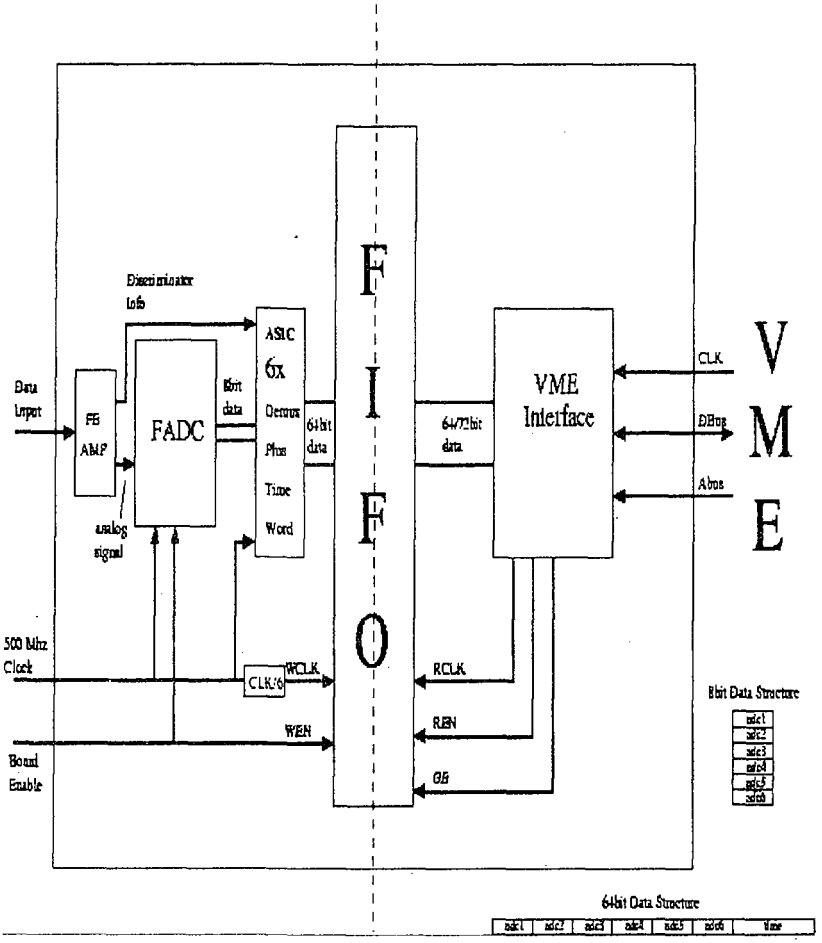

Fig. 13. Block diagram of the waveform digitizer (WFD) with First in First Out (FIFO) memory.

Block diagram of the waveform digitizer (WFD) with First in First Out (FIFO) memory for continuous real-time data acquisition is shown in Fig.13. An analog waveform from the PMT is sent to an 8-bit 500 MHz flash ADC. Every six bytes of flash ADC information (12 ns) are accompanied by a 16 bit time word. The six ADC samples and two bytes of time information are assembled into one 64-bit word by an on-board ASIC. The time word will be latched from a counter on the ASIC, which will be driven, in turn, by the same clock which strobes the flash ADC. The 64 bits of time and ADC

sample information will be written to the FIFO (First in First out) memory at 500/6 MHz. Various control signals will be required to operate the μLan WFD (waveform digitizers).The ASIC will write data to memory only when enabled by a front panel start signal and will cease to write data when it receives a front panel STOP. A VETO input will disable the writing of data without stopping the clock. A RESET input will zero the clock and memory counter. A Control/Status register will be used to control and monitor the board.

The control register will include software emulation of front panel hardware such as START and STOP, so that the board can be operated by a computer alone, as well as bits to set the threshold for the front-end comparator, or to activate or disable zero suppression. The status register will describe the state of the board, including error conditions, the number of data acquisition cycles since RESET, and most importantly, the location of the data pointer in memory. It is planned that. the 50 reguired WEDs will group into five VME crates Each crate will also contain a fast single-board computer running the vxWorks operating system. Approximately 10 times per second, the embedded computer will cycle through all the WFDs in the crate, draining the data from their FIFO buffers. At that point, it will process the data to determine the parameters that describe each pulse. In particular, it will compute the time, area, height, and width of each pulse. The samples for any events which seem to be anomalous in any way will be retained. The remaining data will be forwarded to an event-builder computer.

The total data rate at this stage is less than 10 MBytes per second. It will be feasible to transfer this amount of data over an ordinary 100 MHz Fast Ethernet network to a industry-standard computer running the Linux operating system. This machine would collect the data from the various crates and write it to tape. In fact, it should be possible for it to fill a set of histograms for the pulses which could be fit in a straightforward manner. These histograms would be flushed to tape every minute instead of the entries from which they were made.

It is planned to build and stage the μLan Experiment over a three year period as outlined in this proposal.

6 Measurement of the transverse polarization of positrons from the decay of polarized muons

6.1 Introduction

Measurements of muon decay are low energy tests of standard model. Only a few years ago it has been shown that V-A, as one of the basic assumptions of the standard model, fellows from the results of a selected set of muon decay experiments (including unverse muon decay). The experimental limits obtained up to now, however, still allow for substantial contributions from non-standard couplings. To get better constraints especially for scalar couplings it will improved present limits [67] on the transverse positron polarization by one order of magnitude.

These measurements will yield a more precise of the low energy parameter Mishel η which is needed for a better determination of the Fermi coupling constant. It will also give limits for the time reversal noninvariant component P_T.

6.2 Experiment

The experimental setup [68] is shown in Fig.14. The experiment will be performed at the *PSI* accelerator with a high intensity muon beam. These muons are highly polarized and arrive individual banches every 20 ns at graphite stopping target in the center of a pair of Helmholtz coils. The magnetic field strength chosen so the precession frequency of the stopped muon spins equals the accelerator frequency which is responsible for the time structure mentioned above. This stroboscopic method allows to stop many muons simultaneously.

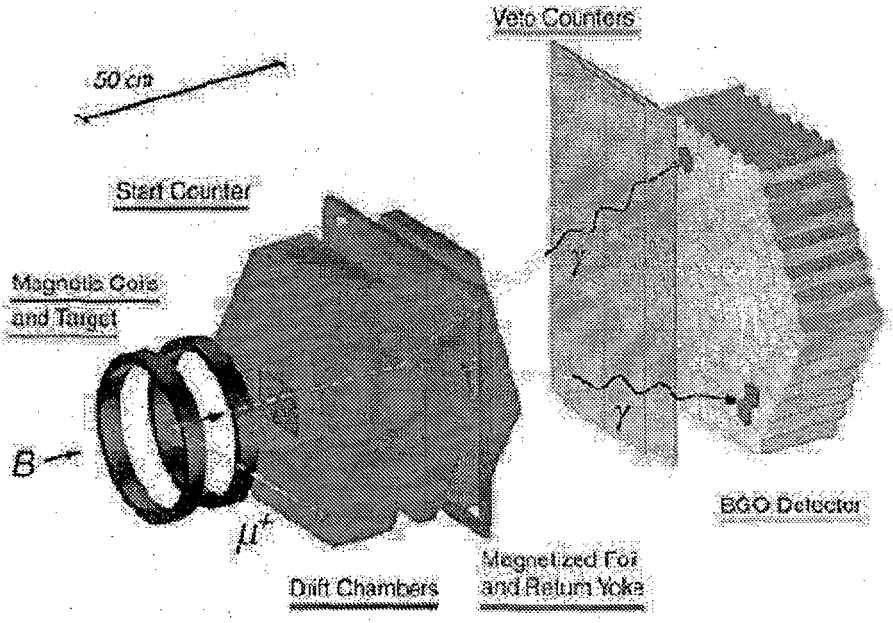

Fig. 14. The experimental setup for measurement of the decay of polarized muons.

In our experiment 200 muons will be in the target at any moment corresponding to a stopping rate of 100/s. Positrons from the decay of these muons and emerging parallel to the field are then detected by a plastic scintillator and a drift chamber array. They then try interaction with polarized electrons in a magnetized iron foil transverse to their line of flight. Annihilation in flight of the decay positrons with the polarized electrons is sensitive to any transverse positron polarization. In that case the resulting two-gamma distribution is not azimuthally isotropic any more. The anisotropy of the gamma quanta will then be measured by an array of 127 BGO counters. The hexagonal drift chamber are able to track the positrons at rates of $3 \cdot 10^6\ s^{-1}$.

It is proposed to use in this experiment the Date Acquisition System based on the

TANDEM [49].

At present the experiment is going on.

7 Conclusion

The most information-rich experiments that are under way or have been performed at the meson factories PSI, TRIUMF, LAMPF, KEK are described above. Structure investigations of various materials with the use of muon spin spectroscopy, investigations of hadron-hadron and hadron-nucleus interactions, and research in physics of exotic systems are also widely carried out at meson factories.

A lot of detectors were used (are used) in all these experiments. The information from the detectors is processed in accordance with certain selection criteria dictated by the structural ideology of the recording electronic system and by physics of the process under investigation.

Improvement of the main parameters of the many-detector systems, such as energy, space, and time resolution of the detectors, multifunctionality and operation speed of data acquisition systems, will allow (due to development of new methods for recording elementary particles and nuclear radiation and upgrading of the data reception and analysis system) an appreciable increase in reliability of the final result that is a goal of particular investigations.

7.1 Acknowledgments

I would like to thank Prof. V.A.Nikitin for very useful discussion and A.Yu.Korzenev for help in manuscript preparation.

Литература

[1] F.C.Frank, Nature 160 (1947) 525.

[2] A.D.Sakharov Report FIAN, M. (1948).

[3] L.W.Alvarez et al., Phys. Rev.105 (1957) 1127.

[4] L.I.Ponomarev, Contemp. Phys. 31 (1990) 219, and references cited therein.

[5] V.M.Bystritsky, Yadernaya Fizika 58 (1995) 808 (Physics of Atomic Nuclei 58 (1995) 746), and references cited therein.

[6] C.Petitjean, in: Proc. 13-th Intern. Conf. On Few Body Problems in Physics, Nucl. Phys. A543 (19920, and references cited therein; G.M.Marshall et al. Hyperfine Interaction 82 (1993) 529; Hyperfine Interaction 118 (1999) 89 and references therein.

[7] V.M.Bystritsky, Yadernaya Fizika 58 (1995) 688 (Physics of Atomic Nuclei 58 (1995) 631) and references cited therein.

[8] V.M.Bystritsky et al., Zh. Eksp. Teor. Fiz. 76 (1979) 460 (Sov. Phys. JETP 49 (1979) 232).

[9] V.M.Bystritsky et al., Phys. Lett. 94B (1980) 476; Pisma Zh. Eksp. Teor. Fiz. 31 (1980) 249; Zh. Eksp. Teor. Fiz.80 (1981) 1700 (Sov. Phys. JETP 53 (1981) 877).

[10] Yu. V. Petrov, Proc. XIV LNPI Winter School, Leningrad, 1979, p.139 (in Russian); Muon Catalyzed Fusion 1 (1987) 351; Muon Catalyzed Fusion 3 (1988) 525 , and references therein.

[11] D.I, Abramov et al., Hyperfine Interactions 119 (1999) 127, and references therein.

[12] Y. Kino et al., Hyperfine Ineractions 101/102 (1996) 325.

[13] A.G.Abrashkevich et al., Hyperfine Interactions 101/102 (1996) 381, and references cited therein.

[14] M. Leon, Hyperfine Interactions 82 (1993) 151 and references therein; J.S. Cohen, Hyp. Inter. 82 (1993) 15 and references therein.

[15] F.Mulhauser et al., PSI Proposal R-98-02 (1998); PSI Annual Scientific Report, 1998. p.21.

[16] A. Del Rosso et al., Hyperfine Interactions 118 (1999) 177.

[17] V.E.Boreiko et al., Nucl. Instr. and Methods A416 (1998) 221.

[18] V.M.Bystritsky and Pen'kov, Yadernaya Fizika 62 (1999) 316(Phys. of Atomic Nuclei 62 (1999) 281).

[19] V.M.Bystritsky et al., Nucl. Instr. and Methods A432 (1999) 188.

[20] S.E.Kuhn et al., Phys. Rev. C 50 (1994) 1771.

[21] Programme PAW, CERN Program Library Long WriteUp 121, Geneva, 1995.

[22] P. Kammel et al., Phys. Lett. 112B (1982) 319; Phys. Rev. A28 (1983) 2611.

[23] W.H.Breunlich et al., Muon Catalyzed Fusion 1 (1987) 67, and references therein

[24] Yu. A. Aristov et al., Yad. Fiz. 33 (1981) 1066 (Sov. J. Nucl. Phys. 33 (1981) 564).

[25] V.M.Bystritsky et al., Zh. Eksp. Teor. Fiz 84 (1983) 1257.

[26] F. Mulhauser et al., Hyperfine Interactions 119 (1999) 35.

[27] J.Wozniak et al., Hyperfine Interactions 119 (1999) 63.

[28] A.Adamczak et al., At. Data Nucl. Tables 62 (1996) 255.

[29] E.M.Maev et al., Hyperfine Interactions 118 (1999) 171.

[30] A. Olin et al., Hyperfine Interaction 118 (1999) 163.

[31] V.B.Belyaev et al., Nucleonika 40 (1995) 85, and references therein.

[32] V.E.Kharchenko et al., Yad.Fiz. 55 (1992) 86.

[33] J.L.Friar et al., Phys.Lett. B251 (1990) 11.

[34] G.Bardin et al., Phys.Lett. 104B (1981) 320; Nucl.Phys. A352 (1981) 365.

[35] V.M.Bystritsky et al. Zh.Eks.Teor.Fiz, 66 (1974) 43 (Sov.Phys. JETP 40 (1974) 811).

[36] A.Bertin et al., Phys.Rev. 8D (1973) 3774.

[37] A.Bertin et al.,Nuovo Cim. 23B (1974) 489.

[38] D.Taggu et al., Hyperfine Inter. 119 (1999) 311; PSI Proposal R-98-03. 1 (1998).

[39] S.L.Glashow, Nucl.Phys. 22 (1961) 579; A.Salam in Elementary Particle Theory: Relativistic Groups and Analiticity Proc. Nobel Symposium, ed. By N.Svartholm (Almquist and Wiksell, Stockholm), nr.8 (1968) 367; S.Weinberg, Phys.Rev.Lett. 19 (1967) 1264; 27 (1971) 1688.

[40] P.Depommier and C.Leroy, Rep.Prog.Phys. 58 (1995) 61.

[41] R.Barbieri et al., Nucl. Phys. B445 (1995) 219.

[42] SINDRUM II Collaboration, PSI Proposal R-87-03, 1987.

[43] F.Muheim, Ph.D.Thesis, Zurich University, 1991.

[44] J.Kaulard, Ph.D.Thesis, RWTH Aachen (1997).

[45] SINDRUM II Collaboration, C.Dohnmen et al., Phys.Lett. B317 (1993) 631.

[46] CES ACC2180 "STARBURST" processor, Creative Electronic Systems SA. 70 Rte. du Pont-Butin, CH-1213 Petit - Lancy (1987).

[47] The GPM general purpose Fastbus Master/ Slave, User Manual, CERN doc.nr.EP85-02 (1985).

[48] CFI service manuals, Dr.B.Struck Company, Hauptstr. 95, D-2000 Tangstadt (1984).

[49] PSI computing division, TANDEM (set of documents).

[50] R.Brun et al., GEANT 3 User's Guide, CERN doc.nr.DD/EE/84-1(1987).

[51] S.Ahmad et al., Phys.Rev. D38 (1988) 2102.

[52] W.Molzon et al., BNL Proposal Experiment MECO, 1999.

[53] D.Pocanic et al., Proposal PSI R89-01.1, 1991.

[54] E.Frlez et al., PSI Annual Report 1997, p.12.

[55] F.Frlez et al ., PSI. Scientific Report v.I, 1998, p.6.

[56] W.K.McFarlane et al., Phys.Rev. D32 (1985) 547.

[57] S.Ritt and P.A.Amaudruz,MIDAS, Program Library of PSI and TRIUMF, 1995.

[58] D.Chang and W.Y.Keung, Phys.Rev.Lett. 62 (1989) 2583.

[59] P.Herczeg and R.N.Mohapatra, Phys.Rev.Lett. 69 (1992) 2475.

[60] A.Halprin and A.Masiero, Phys.Rev. D 48 (1993) R2987.

[61] B.E.Mattias, Phys.Rev.Lett. 66 (1991) 2716.

[62] V.A.Gordeev et al., JETP Lett. 59 (1994) 589.

[63] L.Willmann et al., Phys.Rev.Lett. 82 (1999) 49; PSI Scientific Report v.1, 1998, p.7.

[64] D.R.Gill, V.Selivanov et al., TRIUMF Proposal E 614, 2000.

[65] R.M.Carey et al., PSI Proposal, 2000.

[66] T. van Ritbergen and R.G.Stuart, Phys.Rev.Lett. 82 (1999) 488; Phys.Rev. D 437 (1998) 201.

[67] H.Burkand et al., Phys.Lett., B160 (1985) 343.

[68] K.Bodek et al., PSI Proposal R94-10.1, Collaboration ETH Zurich-PSI-CRACOW-KATOWICE; PSI, Annual Report 1997, Annex I, p14; PSI, Scientific Report 1998, p.8.

Received by Publishing Department
on July 26, 2000.